

PROCEEDINGS OF SPIE

SPIEDigitalLibrary.org/conference-proceedings-of-spie

Retinal SD-OCT image-based pituitary tumor screening

Min He, Weifang Zhu, Xinjian Chen

Min He, Weifang Zhu, Xinjian Chen, "Retinal SD-OCT image-based pituitary tumor screening," Proc. SPIE 10134, Medical Imaging 2017: Computer-Aided Diagnosis, 101343B (3 March 2017); doi: 10.1117/12.2254199

SPIE.

Event: SPIE Medical Imaging, 2017, Orlando, Florida, United States

Retinal SD-OCT image-based pituitary tumor screening

Min He^{1a}, Weifang Zhu^{2a}, Xinjian Chen^{3a*}

^aSchool of Electronics and Information Engineering, Soochow University, Suzhou, Jiangsu Province, 215006, China

ABSTRACT

In most cases, the pituitary tumor compresses optic chiasma and causes optic nerves atrophy, which will reflect in retina. In this paper, an Adaboost classification based method is first proposed to screen pituitary tumor from retinal spectral-domain optical coherence tomography (SD-OCT) image. The method includes four parts: pre-processing, feature extraction and selection, training and testing. First, in the pre-processing step, the retinal OCT image is segmented into 10 layers and the first 5 layers are extracted as our volume of interest (VOI). Second, 19 textural and spatial features are extracted from the VOI. Principal component analysis (PCA) is utilized to select the primary features. Third, in the training step, an Adaboost based classifier is trained using the above features. Finally, in the testing phase, the trained model is utilized to screen pituitary tumor. The proposed method was evaluated on 40 retinal OCT images from 30 patients and 30 OCT images from 15 normal subjects. The accuracy rate for the diseased retina was $(85.00 \pm 16.58)\%$ and the rate for normal retina was $(76.68 \pm 21.34)\%$. Totally average accuracy of the Adaboost classifier was $(81.43 \pm 9.15)\%$. The preliminary results demonstrated the feasibility of the proposed method.

Keywords: Optical Coherence Tomography (OCT), Feature Extraction, Adaboost, Image Processing, Screening, Retinal Segmentation

1. INTRODUCTION

Optical coherence tomography (OCT), first proposed in 1991 by Huang et al.¹, is increasingly used in the ocular diagnosis and management of a variety of diseases, such as glaucoma², diabetic macular edema (DME)³, age-related macular degeneration (AMD)^{4,5}, and so on. It is radiation-free, noninvasive, non-contact, high-speed and high-resolution. An OCT image represents a cross-sectional, micron-scale depiction of the optical reflectance properties of the tissue, which makes most of the anatomical layers of the retina can be quantitatively measured. It is a powerful method to qualitatively assess retinal features and pathologies that has significantly improved our understanding of eye structure and helped in disease diagnosis, treatment and follow-up observation.

Pituitary tumors comprise 12%-15% of all intracranial lesions⁶. 32%-70% of patients with pituitary tumor have the symptom that the tumor compresses the optic nerve, optic chiasma and optic tract, leading to visual loss and retinal nerve fiber layer (RNFL) degeneration. To many patients, visual dysfunction is the initial or the only symptom of pituitary tumor. The OCT technology is the main ophthalmic examination measurement, therefore, the analysis on OCT images is of crucial importance for pituitary tumor screening. However, it is hard to find the retinal differences between normal subjects and patients with pituitary tumors on OCT images directly. Figure 1 (a) shows a B-scan of the OCT image from a pituitary tumor patient, and (b) is a B-scan from a normal subject. Both of them are segmented automatically using our multi-layer graph-search approach, yielding 11 surfaces, in which the red line represents the 1st surface, the pink line means the 6th surface and the blue line stands for the 11th surface⁷. (a) and (b) are quite similar, so it is not easy for doctors to screen the pituitary tumor.

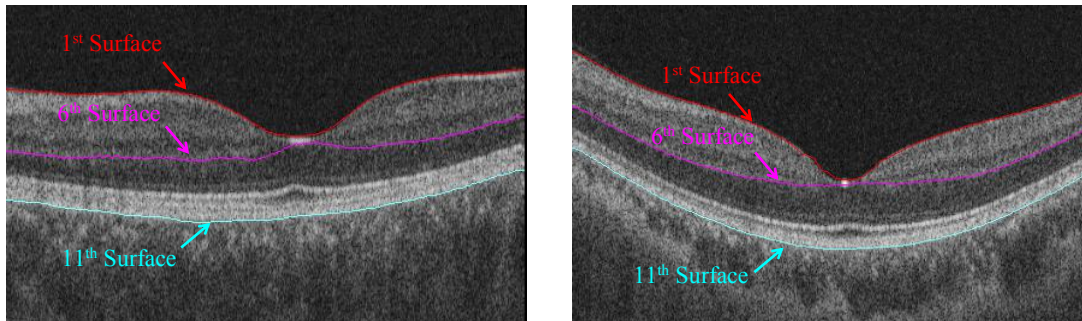
¹ E-mail: hemin1020@foxmail.com; phone (086)15262409520; <http://www.mipav.net>

² E-mail: wfzhu@suda.edu.cn; phone (086)13913199290; <http://www.mipav.net>

³ E-mail: xjchen@suda.edu.cn; phone (086)18260180695; <http://www.mipav.net>

* corresponding author

In this paper, we propose an Adaboost classification based method for automatic pituitary tumor screening. As the first 5 retinal layers (from surface 1 to surface 6) are the most vulnerable in the case of pituitary tumor, they are extracted as the volume of interest (VOI). 19 features, including textural and spatial features are extracted from the VOI. Principal component analysis (PCA) is used to select the primary features, whose contribution rates are up to 95%. Then, an Adaboost based classifier is trained using the above features and tested as a pituitary tumor screener.



(a) A B-scan of a patient's retinal OCT image (b) A B-scan of a normal subject's retinal OCT image

Figure 1. Retinal OCT images of patients with pituitary tumor and normal people.

2. METHODS

The proposed method includes four parts. First, image normalization and noise suppression are performed in the preprocessing step. Second, feature extraction and selection are applied to extract primary spatial and textural features of VOI. Each retinal OCT image generates a feature vector. The feature vectors can represent the input images separately. Third, the labeled feature vectors are used to train the Adaboost based classifier. Finally, the trained classifier is used to screen pituitary tumor. The flowchart of the proposed method is shown in Figure 2. And the details are given below.

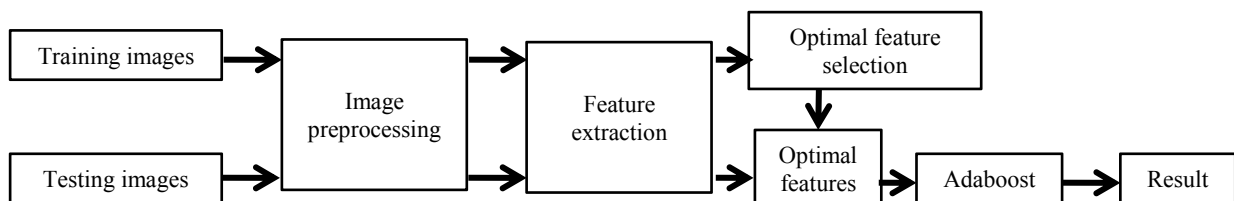


Figure 2. Flowchart of the proposed method used to screen pituitary tumor.

2.1 Preprocessing

The retina is first segmented into 10 layers, using our multi-layer graph-search approach and the first 5 layers are extracted as the VOI. The VOI data is then processed by the following 4 steps: max-min based intensity normalization (S1), down-sampling (S2), slices alignment (S3) and bilateral filter based filtering (S4). S1 normalized the gray level of different OCT images to the same standard by using Formula (1). After normalization, the gray level of each retinal image ranges from 0 to 65535. S2 is used to improve the efficiency of the method. As the original data size is 512*992*256, down-sampling to 512*992*128 would not influence the accuracy distinctly. However, it can reduce the calculation time significantly. In S3, all the other 10 surfaces are aligned based on the 11th surface because the segmentation result of the 11th surface is the most robust. Besides, there is a lot of speckle noise in the OCT image, which may greatly affect the following feature extraction. Therefore, the bilateral filtering is used in S4 to suppress the speckle noise. In a word, S1, S3 and S4 are used to improve the validity of the extracted features and S2 is used to reduce the calculation cost.

$$I_{normalized}(i, j, k) = \frac{I_{original}(i, j, k) - I_{min}}{I_{max} - I_{min}} \times 65535. \quad (1)$$

Where (i, j, k) represents the coordinate of a voxel in VOI, $I_{normalized}(i, j, k)$ represents the value of gray level after normalization, and $I_{original}(i, j, k)$ represents the original gray level of the voxel (i, j, k) . I_{min} and I_{max} are the minimum and maximum values of gray level in VOI respectively.

2.2 Feature extraction and selection

The proposed method is a feature based method to screen pituitary tumor by learning features from VOIs. 19 features are extracted for each VOI, including 9 spatial features and 10 textural features. A vector of features is used to represent each VOI and classification is performed in the feature space.

Spatial features include fovea volume, inner ring volume (inner ring is the region centered on the fovea and its diameter is 3mm), nasal inner retina (from 1st layer to 5th layer) thickness, temporal inner retina thickness, the rate of the peak of nasal inner retina thickness and peak of temporal inner retina thickness, mean, variance, kurtosis and entropy of gray values. All these spatial features are extracted from the VOI. The gray levels used in the spatial features are in the range of [0,65535]. Figure 3 shows the region of fovea and inner ring.

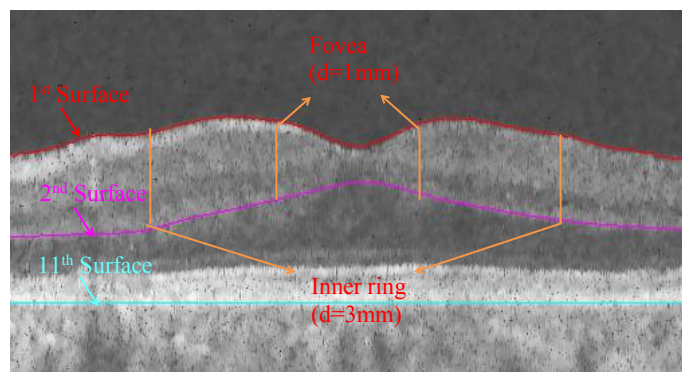


Figure 3. The location of fovea and inner ring. Fovea is the volume with a diameter of 1 mm on the center of the macular from 1st surface to 6th surface. Inner ring is the volume with a diameter of 3 mm on the center of the macular from 1st surface to 6th surface.

Textural features include 3D run length features of 13 directions (including short run emphasis, long run emphasis, gray level non-uniformity, run length non-uniformity and run percentage) and 3D gray level co-occurrence features of 26 directions (including angular second moment, contrast, inverse difference moment, entropy and correlation). Before the textural features are extracted, the original gray level [0, 65535] is mapped to [0, 31] and each VOI is histogram equalized. Figure 4 shows the image after gray level mapping and histogram equalization. PCA is adopted to select the primary features.

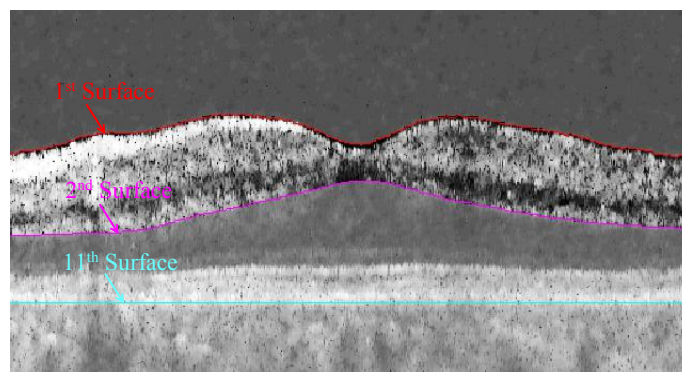


Figure 4. A B-scan from OCT image after gray level mapping and histogram equalization.

A gray level run is defined as a string of consecutive pixels which have the same gray level intensity along a specific linear orientation⁸. A run-length matrix P is defined as: each element P(i,j) represents the number of runs with voxels of gray level equal to i and length of run equal to j along the direction d(x,y,z), where x, y, z are the displacements of the x-axis, y-axis and z-axis. The size of the matrix is M × N, where M is the maximum gray level and N is the possible maximum run length. In 3D OCT image, 13 directions are taken into account, which are listed in Table 1. After constructing the run-length matrix, the features listed in Table 2 are calculated. Their formulas and meaning are also listed in Table 2.

Table 1. Displacement representation of 13 directions used in run-length matrix. Θ is the angle between the projection of the direction on X-Y plane and the X axis. Φ is the angle between the direction and the Z axis.

Number	Direction(θ,Φ)	Vector corresponding to the direction d(x,y,z)
1	(0,90)	(1,0,0)
2	(45,90)	(1,1,0)
3	(90,90)	(0,1,0)
4	(135,90)	(-1,1,0)
5	(0,45)	(1,0,1)
6	(180,45)	(-1,0,1)
7	(90,45)	(0,1,1)
8	(-90,45)	(0,-1,1)
9	(0,0)	(0,0,1)
10	(45,45)	(1,1,1)
11	(135,45)	(-1,1,1)
12	(-45,45)	(1,-1,1)
13	(-135,45)	(-1,-1,1)

Table 2. Features extracted from run-length matrix. Their formulas and meaning are also listed. n_r is the sum of all elements in the matrix. Below is the formula to calculate n_r: $n_r = \sum_{i=1}^M \sum_{j=1}^N P(i, j)$.

Feature of run-length matrix	Formula	What is measured?
Short run emphasis (SRE)	$SRE = \frac{1}{n_r} \sum_{i=1}^M \sum_{j=1}^N \frac{P(i, j)}{j^2}$	Measures the distribution of short runs. The SRE is highly dependent on the occurrence on the short runs and is expected large for fine textures.
Long run emphasis (LRE)	$LRE = \frac{1}{n_r} \sum_{i=1}^M \sum_{j=1}^N P(i, j) * j^2$	Measures the distribution of long runs. The LRE is highly dependent on the occurrence of long runs and is expected large for coarse textures.
Gray level non-uniformity	$GLNU = \frac{1}{n_r} \sum_{i=1}^G \left(\sum_{j=1}^K P(i, j) \right)^2$	Measures the similarity of gray level values. The GLNU is expected small if gray level values are alike in the VOI.

Run length non-uniformity	$RLNU = \frac{1}{n_r} \sum_{j=1}^K \left(\sum_{i=1}^G P(i, j) \right)^2$	Measures the similarity of the length of runs. The RLNU is expected small if the run lengths are alike in the VOI.
Run percentage	$RPC = \frac{n_r}{\sum_{i=1}^M \sum_{j=1}^N P(i, j) * j}$	Measures the homogeneity and the distribution of runs of VOI in a specific direction. The RPC is the largest when the length of runs is 1 for all gray levels in specific direction.

Gray level co-occurrence matrix (GLCM) is one of the most well-known textural analysis methods. Each element $G(i, j)$ in GLCM is the number of occurrences of pair of gray levels i and j , which are a distance \mathbf{d} apart from each other in VOI. The distance \mathbf{d} is defined as voxel distance, can also be replaced by a vector. The value of \mathbf{d} used in this paper is 1. To construct the 3D gray level co-occurrence matrix, the method searches for another pixel in 26 directions, which include the 13 directions listed in Table 1 and their opposite directions. The size of GLCM is $M \times M$, where M is also the maximum gray level. After constructing the co-occurrence matrix, the features listed in Table 3 are calculated. The corresponding formulas and meaning are also listed in Table 3.

Table 3. Features extracted from gray level co-occurrence matrix. Their formulas and meaning are also listed. μ_{col} and μ_{row} are the means of rows and columns of the matrix, σ_{col} and σ_{row} are the standard deviations of the rows and columns of the matrix. Here are the formulas used to calculate μ_{col} , μ_{row} , σ_{col} and σ_{row} : $\mu_{col} = \sum_{i=1}^M \sum_{j=1}^M i \cdot G(i, j)$, $\mu_{row} = \sum_{i=1}^M \sum_{j=1}^M j \cdot G(i, j)$, $\sigma_{col}^2 = \sum_{i=1}^M \sum_{j=1}^M G(i, j) (i - \mu_{col})^2$, $\sigma_{row}^2 = \sum_{i=1}^M \sum_{j=1}^M G(i, j) (j - \mu_{row})^2$.

Feature of gray level co-occurrence matrix	Formula	What is measured?
Angular second moment/Energy	$ASM = \sum_{i=1}^M \sum_{j=1}^M G(i, j)^2$	Measures textural uniformity. Energy reaches its largest value when gray level distribution has either a constant or a periodic form.
Entropy	$ENT = - \sum_{i=1}^M \sum_{j=1}^M G(i, j) \log G(i, j)$	Measures the disorder of VOI and it reaches its maximum when all elements in the matrix are equal. Therefore, entropy is inversely proportional to energy.
Contrast	$CON = \sum_{i=1}^M \sum_{j=1}^M (i - j)^2 G(i, j)$	Measures the amount of local variations in VOI and it reaches higher when there is a frequent occurrence of large gray level occurrence.
Inverse difference moment	$IDM = \sum_{i=1}^M \sum_{j=1}^M \frac{G(i, j)}{1 + (i - j)^2}$	Measures image homogeneity and it reaches its largest value when most of the occurrences in GLCM are concentrated near the main diagonal.
Correlation	$COR = \frac{\sum_{i=1}^M \sum_{j=1}^M ijG(i, j) - \mu_{col}\mu_{row}}{\sigma_{col}\sigma_{row}}$	Measures the degree to which elements of the matrix are concentrated along the main diagonal.

It is worth mentioning that the thickness of RNFL is not selected as a feature, because it's not easy to segment RNFL automatically and correctly in the diseased retina.

2.3 Training

Adaboost is a kind of iterative algorithm. This method allows designers constantly adding new weak classifiers, until it reaches a predetermined margin of small error. Starting with the unweighted training sample, the Adaboost builds a classifier, that produces class labels. If a training data point is misclassified, the weight of that training data is increased (boosted). A second classifier is built using the new weights, which are no longer equal. Again, misclassified training data have their weights boosted and the procedure is repeated. Typically, one may build 500 or 1000 classifiers in this way. A score is assigned to each classifier, and the final classifier is defined as the linear combination of the classifiers from each stage⁹. Adaboost classifier has gained wide popularity in many areas, especially in two-class classification problems, and in this paper it is applied for pituitary tumor screening. All the feature values derived will be sent into classifier to get the training model.

2.4 Testing

In the testing phase, the features of the testing images are as the input to the trained Adaboost classifier for pituitary tumor screening. After classification, each OCT image is assigned a label, according to the result of the label, we get a classification results (1 represents pituitary tumor and 2 represents normal).

3. RESULTS

40 retinal OCT images from 30 patients of pituitary tumor and 30 OCT images from 15 normal subjects were collected by Topcon DRI OCT-1 macula-centered scan in the General Hospital of Nanjing Military Region. The original data size is 512*992*256, and the resolution of each voxel is 11.72μm*2.3μm*23.44μm. 36 images of patients and 27 images of normal subjects were used for training. The rest 4 images of patients and 3 images of normal persons were used for testing. All images were labeled 1 or 2 (1 represents pituitary tumor and 2 represents normal). 10-fold cross validation was adopted in the test. True positive rate (TPR) and true negative rate (TNR) are calculated using formulas (2) and (3), respectively. The accuracy (ACC) for each record is calculated using formula (4). TP, TN, FP, FN represent true positive, true negative, false positive and false negative respectively.

$$TPR = \frac{TP}{TP + FN} \quad (2)$$

$$TNR = \frac{TN}{TN + FP} \quad (3)$$

$$ACC = \frac{TP + TN}{TP + FP + TN + FN} \quad (4)$$

As shown in the Figure 5, the accuracy of the proposed algorithm is around 80%. Table 4 is the average result of ten times test. The TPR of identifying diseased retina is (85.00 ± 16.58)% and the TNR of screening normal retina is (76.68 ± 21.34)%. Totally average accuracy of Adaboost classifier is (81.43 ± 9.15)%. Because the Adaboost classifier is more dependent on the number of samples and sensitive to noisy and outliers, improving data quality and quantity is an effective method to improve the classification accuracy. This is one of our next work.

Table 4. The average ± standard deviation result of 10-fold cross validation.

Classify results \ Ground truth	Abnormal	Normal	Accuracy(%)
Abnormal	3.40±0.66	0.60±0.66	85.00±16.58
Normal	0.70±0.64	2.30±0.64	76.68±21.34

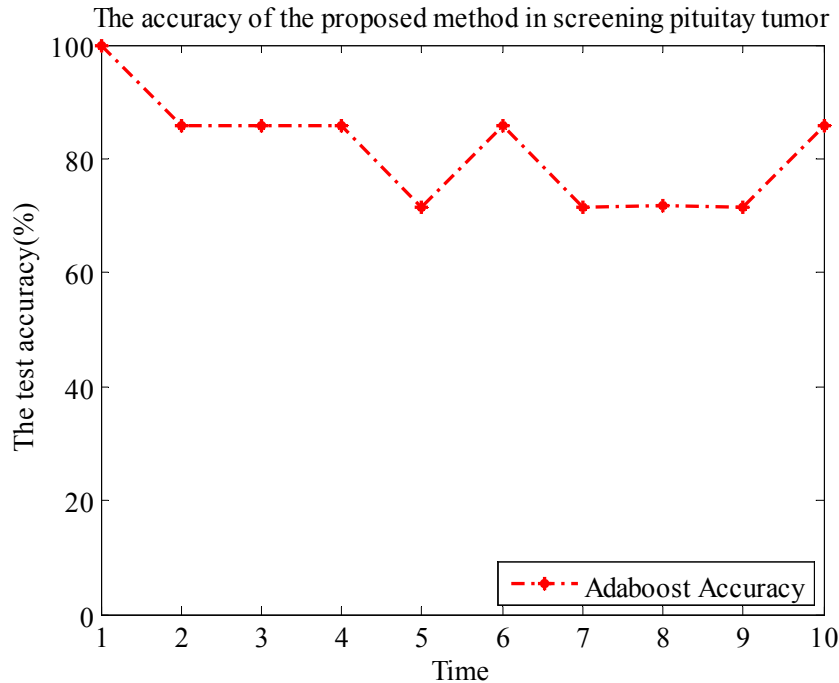


Figure 5. Adaboost accuracy of 10 cross validation. Adaboost accuracy represents the overall detection performance.

4. CONCLUSIONS

In this paper, we first propose an automatic method for the pituitary tumor screening from retinal OCT images. Two new features (fovea volume and inner ring volume) are extracted and other 7 spatial features and 10 textural features are adopted. Adaboost classifier is applied for the classification. The preliminary results show the feasibility of the proposed method. We are going to improve the screening accuracy by enlarging the amount of samples, extracting more features and other methods.

5. ACKNOWLEDGEMENTS

This work was supported in part by the National Basic Research Program of China (973 Program) under Grant 2014CB748600, and in part by the National Natural Science Foundation of China (NSFC) under Grant 81401472, 61622114, 81371629, 61401294, 6140293, and in part by Natural Science Foundation of the Jiangsu Province under Grant BK20140052.

REFERENCES

- [1] Huang D, Swanson E, Lin C, et al, "Optical coherence tomography," *Science*, 254(5035), 1178-1181 (1993).
- [2] Strouthidis N G, Yang H, Fortune B, et al, "Detection of optic nerve head neural canal opening within histomorphometric and spectral domain optical coherence tomography data sets," *Investigative Ophthalmology & Visual Science*, 50(1), 214-223 (2009).
- [3] Hee M R, Puliafito C A, Wong C, et al, "Quantitative assessment of macular edema with optical coherence tomography," *Archives of Ophthalmology*, 113(8), 1019-1029 (1995).

- [4] Ernst B J, Barkmeier A J, Akduman L., "Optical coherence tomography-based intravitreal ranibizumab (Lucentis) for neovascular age-related macular degeneration," *International Ophthalmology*, 30(3), 267-270 (2010).
- [5] Fukuchi T, Takahashi K, Ida H, et al, "Staging of idiopathic choroidal neovascularization by optical coherence tomography," *Graefe's Archive for Clinical and Experimental Ophthalmology*, 239(6), 424-429 (2001).
- [6] Daneshmeyer H V, Wong A, Papchenko T, et al, "Optical coherence tomography predicts visual outcome for pituitary tumors," *Journal of Clinical Neuroscience*, 22(7), 1098-1104 (2015).
- [7] Shi F, Chen X, Zhao H, et al, "Automated 3-D Retinal Layer Segmentation of Macular Optical Coherence Tomography Images With Serous Pigment Epithelial Detachments," *IEEE Transactions on Medical Imaging*, 34(2), 441-452 (2015).
- [8] Donghui X, Kurani A S, Furst J D, et al, "Run-length encoding for volumetric texture," *Visualization, Imaging and Image Processing*, (2004).
- [9] Zhu J, Zou H, Rosset S, et al, "Multi-class AdaBoost," *Statistics & Its Interface*, 2(3), 349-360 (2006).